



Multivariate Taguchi loss function optimization based on principal components analysis and normal boundary intersection

Fabício Alves de Almeida^{1,2} · Ana Carolina Oliveira Santos³ · Anderson Paulo de Paiva¹ ·
Guilherme Ferreira Gomes⁴ · José Henrique de Freitas Gomes¹

Received: 3 June 2020 / Accepted: 20 July 2020 / Published online: 29 July 2020
© Springer-Verlag London Ltd., part of Springer Nature 2020

Abstract

Optimization methods are widely used to improve industrial processes and enhance the quality characteristics of product, where process costs are directly linked. Given this assumption, this study aims to present a multivariate proposal of the Taguchi loss function, to model and optimize manufacturing processes, searching to establish values that prioritize quality and provide the minimum loss in view of the process costs. For this, design of experiments techniques will be used to model the process and the calculated loss functions. The strategy of principal components analysis is used to minimize the data dimension, considering the structure of variance–covariance. Then, the normal boundary intersection method is used to find the Pareto frontier. Based on the values, the method also proposes a total loss function equation, which is characterized as an approach to choose the optimal point based on the sum of the loss functions for the Pareto frontier through the process cost. To demonstrate the behavior of the method, the flux-cored arc welding of stainless-steel cladding process was applied. In view of the results, the method provided an optimal value at the Pareto frontier, contemplating an appropriate balance between minimal loss and higher quality, which were compared with other studies in the literature. The method also provided a reduction in computational effort of approximately 90% (from 210 to 21 subproblems), obtaining the best solution and contemplating the multivariate nature of the data.

Keywords Response surface methodology · Taguchi loss function · Principal component analysis · Normal boundary intersection · Flux-cored arc welding process

1 Introduction

To survive in the competitive industry and meet customer demands, industries should constantly enhance their productive processes. Improvements in quality, cost, flexibility, speed and reliability are frequent challenges faced by the sector. It is possible to find in the literature several articles that present mathematical and computational strategies to

improve quality in industrial processes, such as: [1–5]. On the other hand, the relationship between quality and price is a very important factor since price represents a loss for the consumer at the time of purchase and low quality represents an additional loss during the use of the product. This “loss” includes the cost of customer dissatisfaction that leads to the denigration of the company’s reputation [6, 7]. This concept is very different from traditional guidelines for producers, and includes rework, waste, warranty and services costs as measures of quality.

For these reasons, Taguchi presented the quadratic quality loss function to redefine the quality of a product. All processes that have a decreasing value for the quality loss function (QLF) can assure that performance has been improved. QLF is a mathematical model that accounts for the quality loss in terms of monetary values resulting from the deviation in quality related to the target specification. When analyzing the QLF of a process, the existence of few variables facilitates the calculation. However, an industrial process with

✉ Fabício Alves de Almeida
fabricio.alvesdealmeida@gmail.com

¹ Institute of Industrial Engineering and Management, Federal University of Itajubá, Itajubá, Brazil

² Department of Economics, Faculty of Economic Sciences Southern Minas, Itajubá, Brazil

³ Institute of Integrated Engineering, Federal University of Itajubá, Itabira, Brazil

⁴ Mechanical Engineering Institute, Federal University of Itajubá, Itajubá, Brazil

different combinations of parameters and different quality characteristics can make the analysis difficult. This problem is overcome with the advent of computing, which allows complex mathematical applications aimed at improving quality. The objective in calculating loss is to evaluate quantitatively the loss in quality caused by the variation. This can then be applied to various problems in different sectors such as health, real estate and manufacturing. Even though QLF can be applied in several areas due to its distinct flexibility, these applications are rarely exposed in the literature.

Besides, when analyzing applications aimed at industrial processes, such as welding, there is a need to promote modeling that allows quality optimization, but that considers the cost reduction related to losses. It is possible to verify several studies that use different optimization methods aimed at quality, such as genetic algorithm [4], particle swarm optimization [8], salp swarm algorithm [9], bat optimization algorithm [10] and sunflower optimization [11]. In addition, artificial neural network [12, 13] and normal boundary intersection (NBI) [14] applied to optimization algorithms and damage detection. Among them, the NBI method stands out, given its ability to create Pareto borders that are equidistant and not dominated. However, none of these contemplates the application on QLF.

Another common characteristic of industrial processes is the number of quality variables that impact the industrial cost and, consequently, may present a significant variance–covariance structure. Analyzing data of this nature, there is a need to use multivariate techniques [15]. This type of technique promotes the quality variables interpretation without neglecting the covariance between them. Among the most used multivariate techniques, the principal component analysis (PCA) can be highlighted. PCA is a technique widely used to reduce the dimensionality of extensive and correlated data [16, 17], promoting non-correlated response vectors. This technique can be verified in several applications, such as: [9, 16, 18].

Searching to contemplate the scarcity of QLF applications and contribute to research in this area, this study proposes a multivariate optimization method for the Taguchi loss function. For this, the proposal will merge techniques such as response surface methodology (RSM), ordinary least squares, PCA and NBI in a new methodology to find the best quality index based on the process cost in the face of loss. Based on a priori experimental design, the target value must be found and the loss function of each experiment must be calculated, creating a new loss function experimental matrix. In view of the correlated nature and the data extension, PCA technique is applied, reducing the data dimension (computational effort) and extracting uncorrelated scores. From the modeling of the components scores of loss functions, the multi-objective optimization is performed by the NBI method, creating a frontier of optimal loss function

solutions. In addition, this study presents a total loss function metric to define the best point on the Pareto frontier based on minimizing the QLF. It is important to note that, to the authors' best knowledge, there are no studies in the literature that present a multivariate optimization method for the Taguchi loss function using techniques such as PCA and NBI.

To demonstrate the proposed method in a real case, the flux-cored arc welding (FCAW) of stainless-steel cladding process will be investigated. This approach is characterized by a process of joining metals using the heat of the electric arc set between the wire and the workpiece [19]. FCAW has several quality characteristics that will be investigated in this study, such as bead width, depth of penetration, height of the reinforcement, dilution and productivity. In addition, this process stands out for being widely studied, as in research on [20–24].

This study can be divided as follows: in Sect. 2, the theoretical background is presented, describing techniques such as loss function, RSM, PCA and NBI; Sect. 3 presents the proposed method; the application, method, results and technical discussion of the method is detailed in Sects. 4 and; 5 draws the conclusion.

2 Theoretical background

2.1 Taguchi loss function

Taguchi loss function (or quality loss function) is a method of measuring loss as a result of a service or product that does not satisfy the demanded standards [7]. There are two reasons for using the Taguchi function. Firstly, the characteristics that have different measurement units can be converted into a common magnitude: loss scores. Also, the loss becomes even more significant when the value deviates from the target value, given that the loss of a quadratic function is not linear [25].

On loss modelling, Taguchi also affirms that customers become even more dissatisfied as performance deviates from the target. The author proposed a quadratic function to represent this dissatisfaction, which is defined when the first term derived from the target's Taylor expansion is equal to zero. The curve is centred over the target-value, which represents the best performance. On the other hand, identifying this optimal value is not necessarily a simple task and the designer's best approximation is usually adopted [6].

The Taylor series expansion for the loss function $L(y)=f(y-T)$ around the nominal value is defined as [7]:

$$L(y) = L(T) + \frac{L'(T)}{1!}(y-T) + \frac{L''(T)}{2!}(y-T)^2 + \dots + \frac{L^n(T)}{n!}(y-T)^n \quad (1)$$

Given that $L(y)$ is 0 when $y = T$ (by definition, the loss of quality is zero when $y = T$), and that the function has a minimal value at this point, the first derivative in relation to m is equal to zero. Therefore, the first two terms of Eq. (1) are equal to zero. If the terms of order higher than two are disregarded (truncated at the 2nd order term), the equation is represented as follows:

$$L(y) = \frac{L'(T)}{2!}(y - T)$$

$$L(y) = \delta(y - T)^2, \tag{2}$$

where δ is the proportionality constant. The loss increases significantly as the difference between the real and target values increase, since the loss function is quadratic [7]. This loss is represented by a continuous function, indicating that it is possible to find a minimal point through optimization techniques that corresponds to the lowest losses in a manufacturing process.

2.2 Response surface methodology

Response surface methodology (RSM) is a tool that models, analyses and optimizes problems where the responses can be influenced by several variables. This is also valid where the relationship between these dependent and independent values is unknown [26].

An approximation of the real interaction can be used to analyse a process. The original argument of a multidimensional Taylor Series' expansion can be used to approximate a high order polynomial. This is done by truncating the polynomial in the quadratic term to obtain a second order surface response. In regions where curvatures are present, this model will provide satisfactory results. This model can be expressed in mathematical terms by the Eq. (3), where β represents the coefficients of the model, k represents the number of independent variables being considered and ϵ represents the error. The importance of using this method can be found widely in the literature, where many papers have used the response surface methodology in optimization problems [27, 28].

$$Y(\mathbf{x}) = \beta_0 + \sum_{i=1}^k \beta_i x_i + \sum_{i=1}^k \beta_{ii} x_i^2 + \sum_{i < j} \beta_{ij} x_i x_j + \epsilon. \tag{3}$$

2.3 Principal component analysis

Principal component analysis (PCA) is a multivariate analysis technique used to transform a set of responses or quality

characteristics into a linear relation of the non-correlated components. PCA has three goals: exploration, reduction and data classification. The best results are obtained when the responses or quality characteristics are highly correlated positively and negatively [29].

According to the Johnson and Wichern [30], PCA aims to explain the variance–covariance structure of variables defined through some linear combinations. These authors claim that if the multi-objective functions $f_1(\mathbf{x}), f_2(\mathbf{x}), \dots, f_p(\mathbf{x})$ have correlated response surfaces, they can be written as a random vector $Y^T = [Y_1, Y_2, \dots, Y_p]$. If it is assumed that Σ is the variance–covariance matrix associated with this vector, one has that Σ can be factored into pairs of eigenvalues – eigenvectors $(\lambda_i, e_i), \dots, (\lambda_p, e_p)$, where $\lambda_1 \geq \lambda_2 \geq \dots \geq \lambda_p \geq 0$. Thus, the i_{th} principal component can be given as $PC_i = e_i^T Y = e_1^T Y_1 + e_2^T Y_2 + \dots + e_p^T Y_p$, for $i = 1, 2, \dots, p$.

PCA is often used to reduce the dimensionality of data sets, where they usually have many correlated variables [31]. The number of principal components is less than or equal to the number of original variables and the first few principal components retain most of the variation present in all data [32].

The Kaiser criterion is used to identify the number of principal components needed for the study, where an amount of at least 80% variation is required. In addition, the eigenvalues of the principal components must be greater or equal than 1 [30, 33].

2.4 Normal boundary intersection

In front of a The Normal Boundary Intersection (NBI) is a method capable of finding uniformly equidistant Pareto-optimal solutions [34], compensating for the deficiencies presented in the weighted sum method [35]. This formulation can be written mathematically by Eq. (4):

$$\begin{aligned} & \underset{(\mathbf{x}, t)}{\text{Max}} \quad t \\ \text{S.t.} : & \bar{\Phi} \boldsymbol{\beta} + t \hat{\mathbf{n}} = \bar{\mathbf{F}}(\mathbf{x}) \\ & \mathbf{x} \in \Omega \\ & g_j(\mathbf{x}) \leq 0 \\ & h_j(\mathbf{x}) = 0 \end{aligned} \tag{4}$$

where, Φ presents the *payoff* matrix, obtained by the individual minimization of each objective function; $\bar{\Phi}$ is the scaled *payoff* matrix; $\boldsymbol{\beta}$ refers to the weight vector for each utopia point, and t is a scalar that is perpendicular to the utopia line. $\hat{\mathbf{n}}$ is the normal vector and $\bar{\mathbf{F}}(\mathbf{x})$ represents the vector of the dimensioned objective functions.

NBI represents a line perpendicular to the utopia line (convex hull of individual minima—CHIM) where the normal line is defined by Eq. (5):

$$\vec{r}(t) = [x_0 \ y_0 \ z_0]^T + t \times \vec{\nabla}f[x_0 \ y_0 \ z_0]^T. \tag{5}$$

To create a Pareto frontier, only one point of the surface, as well as the direction vector, is required. In the *payoff* matrix (Φ) and in the scaled *payoff* matrix ($\bar{\Phi}$), the i^{th} line consists of minimum and maximum values of the $f_i(x)$ function, being the lower and upper limits respectively, and also being used.

The Utopia point is the vector which has the individual minimum $\mathbf{f}^U = [f_1^*(x_1^*), \dots, f_i^*(x_i^*), \dots, f_m^*(x_m^*)]^T$. It is the best possible value but is usually outside of the viable solution region [36]. In an antagonistic sense, the Nadir point has the maximum value of each objective function, and is the worst possible solution $\mathbf{f}^N = [f_1^N, \dots, f_i^N, \dots, f_m^N]^T$ [36, 37]. The *payoff* matrices are described by Eq. (6):

$$\Phi = \begin{bmatrix} f_1^*(x_1^*) & \dots & f_1(x_i^*) & \dots & f_1(x_m^*) \\ \vdots & \ddots & \vdots & \ddots & \vdots \\ f_i(x_1^*) & \dots & f_i^*(x_i^*) & \dots & f_i^*(x_m^*) \\ \vdots & \ddots & \vdots & \ddots & \vdots \\ f_m(x_1^*) & \dots & f_m(x_i^*) & \dots & f_m^*(x_m^*) \end{bmatrix} \Rightarrow \bar{\Phi} = \begin{bmatrix} \bar{f}_1^*(x_1^*) & \dots & \bar{f}_1(x_i^*) & \dots & \bar{f}_1(x_m^*) \\ \vdots & \ddots & \vdots & \ddots & \vdots \\ \bar{f}_i(x_1^*) & \dots & \bar{f}_i^*(x_i^*) & \dots & \bar{f}_i^*(x_m^*) \\ \vdots & \ddots & \vdots & \ddots & \vdots \\ \bar{f}_m(x_1^*) & \dots & \bar{f}_m(x_i^*) & \dots & \bar{f}_m^*(x_m^*) \end{bmatrix}, \tag{6}$$

where: $\bar{f}_i(\mathbf{x}) = \begin{bmatrix} f_i(\mathbf{x}) - f_i^U \\ f_i^N - f_i^U \end{bmatrix} = \begin{bmatrix} f_i(\mathbf{x}) - f_i^l \\ f_i^{\text{MAX}} - f_i^l \end{bmatrix}$.

Therefore, for bi-objective problems, the NBI formulation of Eq. (4) can be rewritten as the Eq. (7):

$$\left\{ \begin{array}{l} \text{Min}_{\mathbf{x}} \quad F(\mathbf{x}) = \bar{f}_1(x) \\ \text{St. :} \quad \bar{f}_1(\mathbf{x}) - \bar{f}_2(\mathbf{x}) + 2\beta_1 - 1 = 0 \\ \quad \quad \quad \mathbf{x} \in \Omega. \\ \quad \quad \quad g_j(\mathbf{x}) \leq 0 \\ \quad \quad \quad h_{j+1}(x) = 0 \end{array} \right. \tag{7}$$

3 NBI PCA-based multivariate Taguchi loss function optimization

Many studies use optimization approaches to improve product quality (as inferred in Sect. 1), in addition to reducing costs and losses during the process. When checking these industrial processes, it is possible to find a significant correlation between the quality responses, bringing the need to

use appropriate techniques to treat these data. Therefore, this study proposes a multivariate approach to the Taguchi loss function using PCA and the NBI optimization technique. The method can be divided into five steps, illustrated in Fig. 1 and described below.

- Step 1. Faced with a suitable design of experiments (DOE), such as RSM, an experimental matrix can be created for the process under analysis. The experimental lines must be generated randomly, so that there is no bias. Thus, it is possible to collect all responses to the process, such as quality characteristics, sustainability, among others, in addition to the process cost.
- Step 2. After collecting all the responses, the loss function must be calculated. For that, it is necessary to find the utopian value for each of the response. These values can be provided by the customer or through individual optimization for each quality response (for the application of this study, individual optimization will be

considered). Based on this, it is possible to calculate (from Eq. (2)) the values of the loss functions for each DOE line.

- Step 3. Based on the new experimental matrix [considers the values of loss functions (L_i)], one must analyze the degree of correlation between these values. If the responses have a significant variance–covariance structure, a multivariate strategy must be used, such as PCA. Hence, the necessary number of components is verified using the Kaiser criterion as presented in Sect. 2.3. After that, the principal components scores must be extracted.
- Step 4. Considering the loss functions component scores (L_{PCi}), the DOE should be modeled and analyzed again based on these scores, calculating the coefficients necessary to perform the multi-objective optimization. For this, the NBI method must be used, which is capable of generating Pareto frontiers based on different weight distributions for the restrictions (detailed in Sect. 2). This step allows to find the real optimal values for the quality responses based on the loss functions.
- Step 5. From the Pareto frontier of the original responses, the loss functions are recalculated, considering the

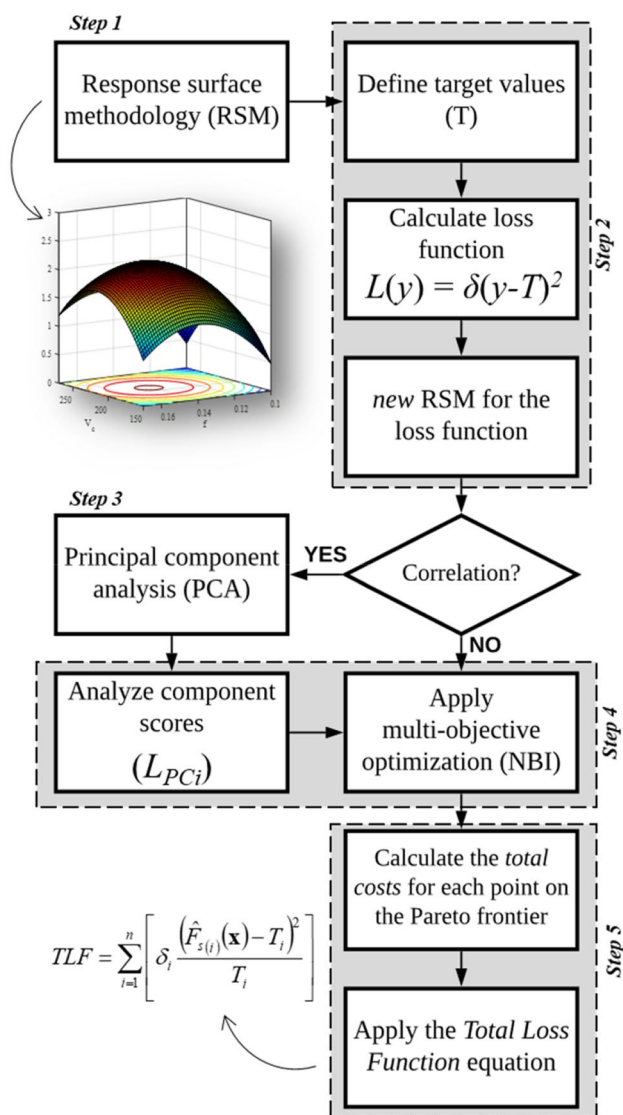


Fig. 1 Flowchart of the multivariate Taguchi loss function optimization approach

costs of each parameter. To carry out this step, the modeling of total costs must be formulated (such as labor, materials, energy, etc.). After that, the respective values must be found for each point on the Pareto frontier. This allows to obtain the loss value for each quality response.

As a criterion for decision making, the best point can be found according to Eq. (8), indicating the value that has the

lowest total loss, indicated at the Pareto frontier. In this sense, this equation considers the sum of all loss functions (of the responses of interest) for each machine parameter, associated with their respective total cost (δ). The point with the lowest loss value is characterized as the best point on the Pareto frontier. This metric is called a total loss function (TLF).

$$TLF = \sum_{i=1}^n \left[\delta_i \frac{(\hat{F}_{s(i)}(\mathbf{x}) - T_i)^2}{T_i} \right] \tag{8}$$

4 A case study of flux-cored arc welding (FCAW) of stainless-steel cladding process

4.1 FCAW process modeling

To apply the proposed method in a real case, the flux-cored arc welding of stainless-steel cladding process will be investigated. Experiments were carried out using an ESAB AristoPower 460 welding machine, an AristoFeed 30-4-watt MA6 module (employed to feed the wire), and a mechanical system device to control welding speed, torch distance and torch angle, which was defined as 15° to “pushing”. The base metal was AISI 1020 carbon steel cut into plates of 120 × 60 × 6.35 mm. Filler metal was a flux-cored stainless-steel wire type AWS E316LT1-1/4, with a diameter of 1.2 mm and linear density of 7.21 g/m. Chemical compositions of the materials are presented in Table 1. To carry out this study, *Minitab*®, *Matlab*® and *Visual Basic for Applications (VBA)*® were used.

A mixture of 75% Ar + 25% CO₂ was used as the shielding gas at a flow rate of 16 L/min. The welding technique used in the experiments was bead on plate, setting the input variables according to the chosen DOE. Input variables were wire feed rate (W_f), voltage (V), welding speed (S) and the distance from the contact tip to the work piece (N).

Based on the steps described in Sect. 3, experiments based on the DOE technique should initially be performed. Following a Central Composite Design (CCD), 31 experiments were carried out: 16 factorial points ($2^k = 2^4$), eight axial points ($2k = 2 \times 4$) and seven center points. The parameter levels were established based on previous tests and are presented in Table 2.

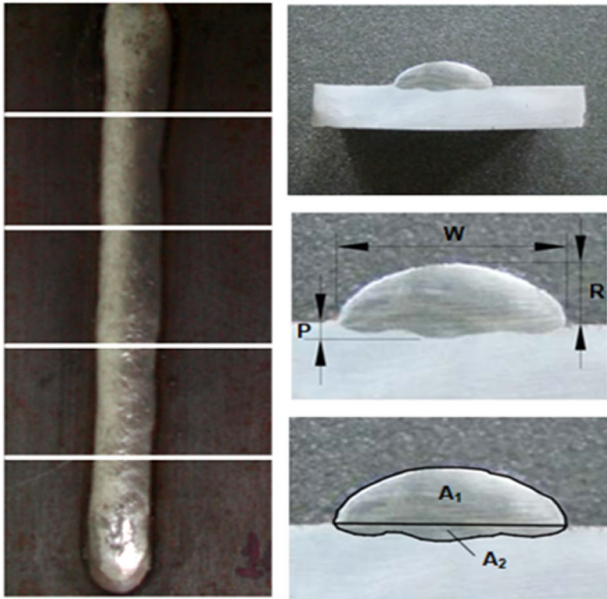
The samples were cut at four different points along the specimens (Fig. 2) and their cross sections were attacked with nital solution (4%) and then photographed. The

Table 1 Chemical composition of base metal and filler metal [23]

Material	C [%]	Mn [%]	P [%]	S [%]	Si [%]	Ni [%]	Cr [%]	Mo [%]
AISI 1020	0.18–0.23	0.30–0.60	0.04	0.05	–	–	–	–
AWS E316LT1-1/4	0.03	1.58	–	–	1.00	12.4	18.5	2.46

Table 2 Input variables and levels [23]

Parameter	Unit	Notation	Levels				
			-2	-1	0	1	2
Wire feed rate	[m/min]	W_f	5.5	7	8.5	10	11.5
Voltage	[Volt]	V	24.5	27	29.5	32	34.5
Welding speed	[cm/m]	S	20	30	40	50	60
Distance from contact tip to work piece	[mm]	N	10	15	20	25	30

**Fig. 2** Welding bead, cross sectional weld bead profile and Bead geometry

software *Analysis Five*[®] was used to measure the bead width (W), penetration (P), reinforcement (R), penetration area (A_2) and total area ($A_t = A_1 + A_2$) of the weld, as shown in Fig. 2. Then, the dilution percentage (D) was obtained by calculating A_2/A_t . In addition, the percentage of productivity (PI) was calculated, as described in Gomes et al. [23]. Table 3 presents the results of the experiments regarding the measured responses. In addition, this table also describes the electric current (I) values measured for each experimental parameter. These values will later be used to calculate the energy costs of the process.

4.2 Multivariate Taguchi loss function optimization for FCAW process

Considering the quality responses, it is possible to verify that the experimental design from the general second order

polynomial model (step 1) presented in Eq. (3). The coefficients were estimated using the ordinary least squares algorithm and are described in Table 4. In view of the original responses of the process, it is possible to verify that they all present an appropriate adjustment (R_{adj}^2), as detailed in Table 4. Furthermore, it is possible to define the individual optimum to calculate the loss function of the responses (step 2). Considering the characteristics of the welding process, the characteristics W , R and PI must be maximized, while P and D must be minimized [23]. In this sense, the utopian values of each response were found, with $\mathbf{Y}^* = [15.570 \text{ mm}; 0.830 \text{ mm}; 3.340 \text{ mm}; 16.3\%; 100\%]$ for W , P , R , D and PI , respectively.

In view of the optimum points and Eq. (2), it is possible to generate a new experimental design for the loss functions of FCAW process (In this initial stage, a δ value equal to 1 was considered). While Table 5 presents the values of the loss functions, Table 6 presents the variance–covariance structure of the loss function values. As a result, the PCA strategy was applied to extract the component scores that adequately represent all the analyzed values. In view of the Kaiser criterion (highlighted in step 3), Fig. 3 presents the Pareto Chart for the principal components of the loss functions, where it is possible to verify that two components (L_{PC1} and L_{PC2}) are necessary to represent the entire data set (eigenvalues greater than 1 and explanation percentage equal to 81.6%).

From the RSM, it is possible to estimate the coefficients of the experimental design based on the loss function, represented by the principal components. The regression equations are described in Eqs. (9) and (10), showing high adjustment values with R_{adj}^2 equal to 93.89% and 94.39% for L_{PC1} and L_{PC2} , respectively. To graph the behavior of the equations mentioned above, Fig. 4 and 5 illustrate the response surface plots (in addition to the contour plot) for L_{PC1} and L_{PC2} , respectively. From these graphs, it is possible to verify that L_{PC2} presents a more linear behavior when comparing with L_{PC1} . It is important to note that the parameters that do not appear on the axes were fixed in their respective center point. Both Figures show the possible combinations between the control variables. Figure 6 illustrates the main effects of

Table 3 Experimental matrix and electric current values. Adapted from [23]

Run	Input variables				Responses					
	W_f	V	S	N	W	P	R	D	PI	I
	[m/min]	[Volt]	[cm/min]	[mm]	[mm]	[mm]	[mm]	[%]	[%]	[A]
1	7.0	27.0	30.0	15.0	11.2	1.3748	2.6278	26.44	89.74	172
2	10.0	27.0	30.0	15.0	13.0	1.6609	3.1158	25.82	89.71	214
3	7.0	32.0	30.0	15.0	12.7	1.6891	2.4963	31.49	89.14	181
4	10.0	32.0	30.0	15.0	15.0	1.9768	2.7782	31.25	89.47	233
5	7.0	27.0	50.0	15.0	9.2	1.6468	2.1651	36.22	91.58	173
6	10.0	27.0	50.0	15.0	10.0	1.9361	2.6666	33.69	90.70	205
7	7.0	32.0	50.0	15.0	9.7	1.5379	2.0649	37.12	87.43	176
8	10.0	32.0	50.0	15.0	11.5	2.1808	2.4249	41.08	88.36	218
9	7.0	27.0	30.0	25.0	10.3	1.2504	2.8700	22.46	90.49	143
10	10.0	27.0	30.0	25.0	11.4	0.9993	3.5940	18.32	89.47	179
11	7.0	32.0	30.0	25.0	11.3	1.3215	2.8479	23.71	90.60	152
12	10.0	32.0	30.0	25.0	13.3	1.1005	3.1793	21.96	89.81	179
13	7.0	27.0	50.0	25.0	8.0	1.1114	2.5543	24.96	94.03	143
14	10.0	27.0	50.0	25.0	8.6	1.2254	2.7967	23.31	90.17	177
15	7.0	32.0	50.0	25.0	8.5	1.3697	2.3628	28.77	93.52	151
16	10.0	32.0	50.0	25.0	10.8	1.6370	2.5983	30.19	91.74	183
17	5.5	29.5	40.0	20.0	9.1	1.3822	2.2068	31.56	92.62	141
18	11.5	29.5	40.0	20.0	12.2	2.1393	3.0557	30.95	89.52	213
19	8.5	24.5	40.0	20.0	9.4	1.2045	3.0263	22.84	90.41	175
20	8.5	34.5	40.0	20.0	11.7	1.8644	2.4578	35.58	90.04	188
21	8.5	29.5	20.0	20.0	14.9	0.9476	3.4536	18.58	90.27	187
22	8.5	29.5	60.0	20.0	8.5	1.4328	2.2498	35.78	93.08	172
23	8.5	29.5	40.0	10.0	11.7	2.1784	2.6103	40.44	88.15	223
24	8.5	29.5	40.0	30.0	9.2	1.2825	2.8912	24.16	92.05	152
25	8.5	29.5	40.0	20.0	10.8	1.7082	2.5960	31.05	93.04	180
26	8.5	29.5	40.0	20.0	10.9	1.7229	2.5923	31.67	91.91	181
27	8.5	29.5	40.0	20.0	10.7	1.6230	2.6549	30.88	92.51	179
28	8.5	29.5	40.0	20.0	10.6	1.8014	2.4950	32.83	91.98	176
29	8.5	29.5	40.0	20.0	10.6	1.4854	2.6208	29.99	92.15	175
30	8.5	29.5	40.0	20.0	10.6	1.4897	2.6119	31.09	92.40	172
31	8.5	29.5	40.0	20.0	10.6	1.5041	2.5574	31.02	92.58	174

the components in relation to the parameters, considering the significant relationships for a 95% confidence interval. In Fig. 6a, it can be seen that the values of L_{PC1} increase as

the parameters W_f , V and S increase, showing an inverse behavior for parameter N . However, when analyzing Fig. 6b, the effects of W_f and S have opposite meanings for L_{PC2} , while V and N have a lesser effect in the center point region.

$$\begin{aligned}
 L_{PC1} = & 6.4 - 2.217 \times W_f - 0.259 \times V - 0.020 \times S + 0.381 \times N + 0.0716 \times W_f \times W_f + 0.0069V \times V \\
 & - 0.001486 \times S \times S + 0.01024 \times N \times N + 0.0313 \times W_f \times V + 0.01186 \times W_f \times S \\
 & - 0.0069 \times W_f \times N + 0.00776 \times V \times S - 0.02230 \times V \times N - 0.00822 \times S \times N
 \end{aligned}
 \tag{9}$$

Table 4 Model coefficients for the RSM

Coef.	<i>W</i>	<i>P</i>	<i>R</i>	<i>D</i>	PI
Constant	10.6996	1.6193	2.5898	0.3122	0.9237
W_f	0.7967	0.1221	0.2026	-0.0028	-0.0055
<i>V</i>	0.6555	0.1220	-0.1156	0.0249	-0.0027
<i>S</i>	-1.4507	0.0934	-0.2618	0.0368	0.0061
<i>N</i>	-0.6290	-0.2408	0.1261	-0.0425	0.0090
W_f^2	-0.0033	0.0266	0.0025	-0.0023	-0.0039
V^2	-0.0240	-0.0300	0.0302	-0.0074	-0.0060
S^2	0.2637	-0.1161	0.0576	-0.0125	-0.0024
N^2	-0.0440	0.0190	0.0323	0.0003	-0.0063
$W_f \times V$	0.2663	0.0337	-0.0467	0.0077	0.0028
$W_f \times S$	-0.1137	0.0757	-0.0304	0.0050	-0.0026
$W_f \times N$	-0.0308	-0.0998	-0.0061	-0.0042	-0.0049
$V \times S$	-0.1023	0.0002	0.0109	0.0023	-0.0032
$V \times N$	-0.0064	0.0048	-0.0010	-0.0020	0.0055
$S \times N$	0.0665	0.0045	-0.0302	-0.0077	0.0057
R^2_{adj}	97.98%	83.24%	92.81%	93.43%	84.77%

$$\begin{aligned}
 L_{PC2} = & 29.8 + 0.069 \times W_f - 1.495 \times V - 0.276 \times S - 0.249 \times N + 0.0151 \times W_f \times W_f \\
 & + 0.02680 \times V \times V + 0.000456 \times S \times S + 0.00637 \times N \times N - 0.0106 \\
 & - W_f \times V + 0.01267 \times W_f \times S + 0.0005 \times W_f \times N + 0.00014 \times V \times S \\
 & - 0.00055 \times V \times N + 0.00021 \times S \times N.
 \end{aligned} \tag{10}$$

From these coefficients, it is possible to perform multi-objective optimization using the NBI method (step 4). For this, the two principal components were considered, where they present different optimization directions. Concerning the original responses and their respective optimization directions, the behavior of the loss function components was analyzed to define the appropriate approach. In this sense, it is possible to verify that L_{PC1} presents a greater degree of explanation of the characteristics that need to be minimized. (*P* and *D*). However, when analyzing L_{PC2} , it appears that this component explains the characteristics that should be maximized (*W*, *R* and PI). In this sense, L_{PC1} must be minimized, while L_{PC2} needs to be maximized. Figure 7 illustrates the level of similarity between the original quality characteristics and the principal components for loss function, where Ward linkage method was used, considering the absolute correlation. Then, it was possible to calculate the

individual optimal values for each component and find the *payoff* matrix for the NBI method, according to Eq. (11).

$$\Phi = \begin{bmatrix} -2.599 & -1.1824 \\ -1.8911 & 2.4985 \end{bmatrix}. \tag{11}$$

In view of the criteria established by the NBI method, the distribution of weights to create the constraints (necessary when forming the Pareto frontier) was formulated using the Simplex-Lattice mixture-design. Thus, it was possible to create a total of 21 different weight combinations. The importance of using the PCA also stands out here, because without reducing the data dimension, the optimization method would need 210 subproblems to contemplate the weight distribution for the 5 original responses. Applying the NBI method, it was possible to find 21 distinct optimal, where all represent optimal Pareto points. Table 7 presents the values found for the frontier, with the optimal values of the components and the real values of the processes.

4.3 Optimal point selection using the total loss function

Choosing the best point on a Pareto frontier is not a trivial task. In this sense, to find the best point on the frontier, one must recalculate the loss functions considering the optimal Pareto values. That is, it is possible to find the cost of the FCAW process for each point of the Pareto frontier, from the machine parameters. The FCAW process cost (C_t) was calculated based on Marques et al. [19] and is described, for each line on the Pareto border, in Table 7. In this work, C_t included machine and labor (C_{ml}), filler metal and flux (C_{mf}), gas (C_g) and energy (C_e), as shown in Eq. (12). Additional information to estimate process costs is described in Table 8, based on machine parameters. Table 9 presents the equations used to calculate the components of C_t .

$$C_t = C_{ml} + C_{mf} + C_g + C_e. \tag{12}$$

Table 5 Experimental matrix of the loss function values and component scores

Run	Input variables				Loss function							
	W_f	V	S	N	L_W	L_P	L_R	L_D	L_{PI}	L_{PC1}	L_{PC2}	
1	7.0	27.0	30.0	15.0	19.1844	0.2916	0.5041	0.0095	0.0105	-0.43032	0.75705	
2	10.0	27.0	30.0	15.0	6.6564	0.6889	0.0484	0.0095	0.0106	0.00671	1.99333	
3	7.0	32.0	30.0	15.0	8.2369	0.7396	0.7056	0.0217	0.0118	1.01984	0.80900	
4	10.0	32.0	30.0	15.0	0.2704	1.3225	0.3136	0.0217	0.0111	1.51866	1.69457	
5	7.0	27.0	50.0	15.0	40.4496	0.6724	1.3689	0.0389	0.0071	0.72193	-2.40873	
6	10.0	27.0	50.0	15.0	31.4721	1.2321	0.4489	0.0314	0.0086	0.95287	-0.25409	
7	7.0	32.0	50.0	15.0	33.8724	0.5041	1.6384	0.0430	0.0158	2.14319	-1.64672	
8	10.0	32.0	50.0	15.0	16.4836	1.8225	0.8464	0.0612	0.0135	3.89315	-0.28239	
9	7.0	27.0	30.0	25.0	27.5625	0.1764	0.2209	0.0033	0.0090	-1.30334	0.80653	
10	10.0	27.0	30.0	25.0	17.1396	0.0289	0.0625	0.0003	0.0111	-1.20325	1.75119	
11	7.0	32.0	30.0	25.0	18.4900	0.2401	0.2401	0.0060	0.0088	-0.98555	1.06106	
12	10.0	32.0	30.0	25.0	4.9729	0.0729	0.0256	0.0033	0.0104	-0.94131	2.14824	
13	7.0	27.0	50.0	25.0	57.4564	0.0784	0.6241	0.0076	0.0036	-2.32197	-1.73693	
14	10.0	27.0	50.0	25.0	48.3025	0.1600	0.2916	0.0045	0.0097	-1.52458	-0.08149	
15	7.0	32.0	50.0	25.0	50.2681	0.2916	0.9604	0.0162	0.0042	-1.35592	-2.05629	
16	10.0	32.0	50.0	25.0	22.3729	0.6561	0.5476	0.0189	0.0068	-0.20680	-0.03677	
17	5.5	29.5	40.0	20.0	42.2500	0.3025	1.2769	0.0247	0.0054	-0.53649	-2.25872	
18	11.5	29.5	40.0	20.0	11.2896	1.7161	0.0784	0.0217	0.0110	1.62826	1.63945	
19	8.5	24.5	40.0	20.0	37.8225	0.1369	0.0961	0.0045	0.0092	-1.53593	0.57655	
20	8.5	34.5	40.0	20.0	15.0544	1.0609	0.7744	0.0389	0.0099	1.68328	-0.12793	
21	8.5	29.5	20.0	20.0	0.4096	0.0144	0.0121	0.0007	0.0095	-1.15370	2.29285	
22	8.5	29.5	60.0	20.0	50.2681	0.3600	1.1881	0.0389	0.0048	-0.23149	-2.81972	
23	8.5	29.5	40.0	10.0	14.7456	1.8225	0.5329	0.0563	0.0140	3.63868	0.42697	
24	8.5	29.5	40.0	30.0	40.3225	0.2025	0.2025	0.0060	0.0063	-1.78807	-0.04533	
25	8.5	29.5	40.0	20.0	22.5625	0.7744	0.5476	0.0217	0.0048	-0.24103	-0.32543	
26	8.5	29.5	40.0	20.0	21.5296	0.7921	0.5625	0.0247	0.0065	0.15228	-0.17324	
27	8.5	29.5	40.0	20.0	23.3289	0.6241	0.4761	0.0217	0.0056	-0.36252	-0.17142	
28	8.5	29.5	40.0	20.0	24.6016	0.9409	0.7056	0.0280	0.0064	0.45242	-0.58315	
29	8.5	29.5	40.0	20.0	24.3049	0.4356	0.5184	0.0189	0.0062	-0.60256	-0.16616	
30	8.5	29.5	40.0	20.0	24.8004	0.4356	0.5329	0.0217	0.0058	-0.55156	-0.31446	
31	8.5	29.5	40.0	20.0	25.0000	0.4489	0.6084	0.0217	0.0055	-0.53488	-0.46781	

Table 6 Correlation analysis for the loss function values

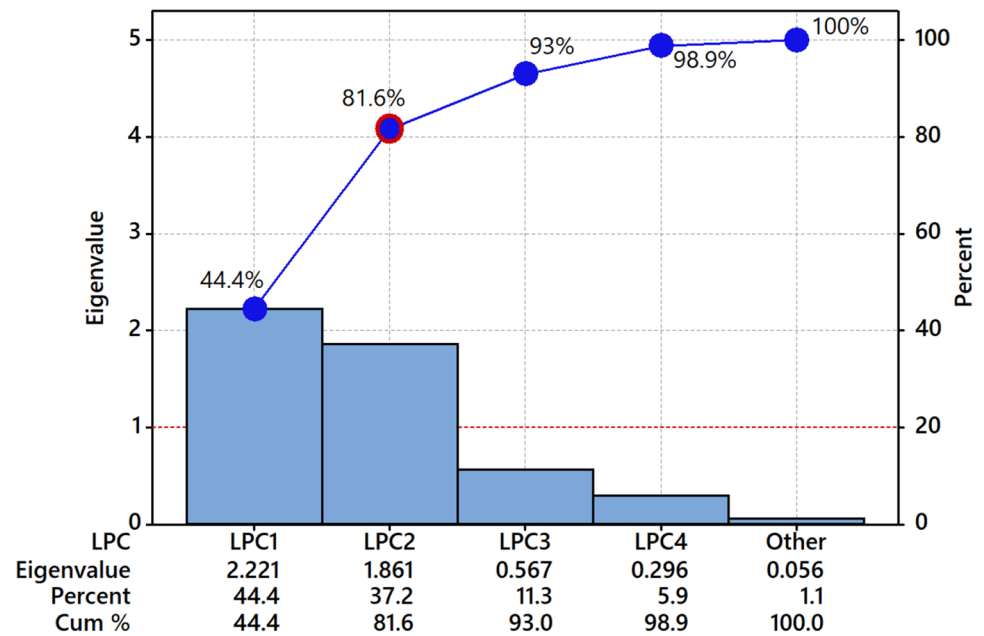
	L_W	L_P	L_R	L_D
L_P	-0.372 ^a 0.039 ^b			
L_R	0.479 ^a 0.006 ^b	0.114 ^a 0.542 ^b		
L_D	0.013 ^a 0.945 ^b	0.747 ^a 0.000 ^b	0.662 ^a 0.000 ^b	
L_{PI}	-0.533 ^a 0.002 ^b	0.402 ^a 0.025 ^b	-0.098 ^a 0.601 ^b	0.266 ^a 0.148 ^b

^aPearson correlation

^bP value

Under previous information presented (and also the Eq. (8)), it is possible to find the total loss function value (step 5). This value includes the total loss, for all quality responses in relation to the cost of each machine parameter. So, to find the best point on the Pareto frontier, just find the lowest total loss function value, which represents the lowest loss for the process. For this, the total cost is calculated, with the factor δ , for each point on the Pareto frontier. Subsequently, Eq. (8) is applied to find the minimum “total loss” value. Table 10 presents the cost and the loss values for the Pareto solution, in addition to the TLF values, indicating the optimal point of the frontier. Therefore, it can be

Fig. 3 Pareto chart and number of principal components for loss function



inferred that the best point on the border is represented by line 2, with parameters $\mathbf{X} = [9.43; 28.89; 21.18; 20.56]$ for W_f , V , S and N , respectively. Such a configuration represents the values $\mathbf{Y} = [14.655 \text{ mm}; 0.959 \text{ mm}; 3.511 \text{ mm}; 18.03\%; 89.94\%]$ for W , P , R , D and PI , respectively, being the optimal response in relation to the Pareto frontier. Figure 8 illustrates the relationship of TLF with the values found in the optimization of the multivariate loss functions (L_{PC1} and L_{PC2}). The red dot highlights the optimal value found.

4.4 Comparison of results through the TLF approach

To compare the results with another study already mentioned in the literature, the results found in Gomes et al. [23] were investigated. In this study, the authors performed a direct optimization for the FCAW process. For this, they mixed the PCA technique with the mean square error approach (MMSE). To analyze and compare the results found by the authors, an analysis of the process costs was carried out from the machine parameters to the optimum point found by Gomes et al. [23]. The MMSE method provided machine parameter values of $W_f = 10.31$ [m/min]; $V = 26.97$ [Volt]; $S = 50.33$ [cm/min]; $N = 23.36$ [mm]. For these reasons, it

was possible to apply the TLF decision-making approach, described in Eq. (8). Table 11 presents the information and calculations of the optimal points found for both studies, in addition to the cost information and the total loss function values.

From this, it is possible to verify that the optimum point found in the study by Gomes et al. [23] presented a cost of US\$ 5.30, presenting a final value of TLF equal to 4.7011. However, the method proposed in this study showed a lower total loss value (TLF = 1.0521), proving to be a better option for this process. In other words, when analyzing the results of both studies, it appears that the multivariate method Taguchi loss function optimization (proposed in this work) provided results closer to the targets established. In addition, the method of this study considers the relationship established by the process cost, promoting results in a scope closer to the industrial reality.

5 Conclusion

This study presents a multivariate proposal to find the combination of parameters to minimize the total quality values based on cost and loss functions. This proposal includes

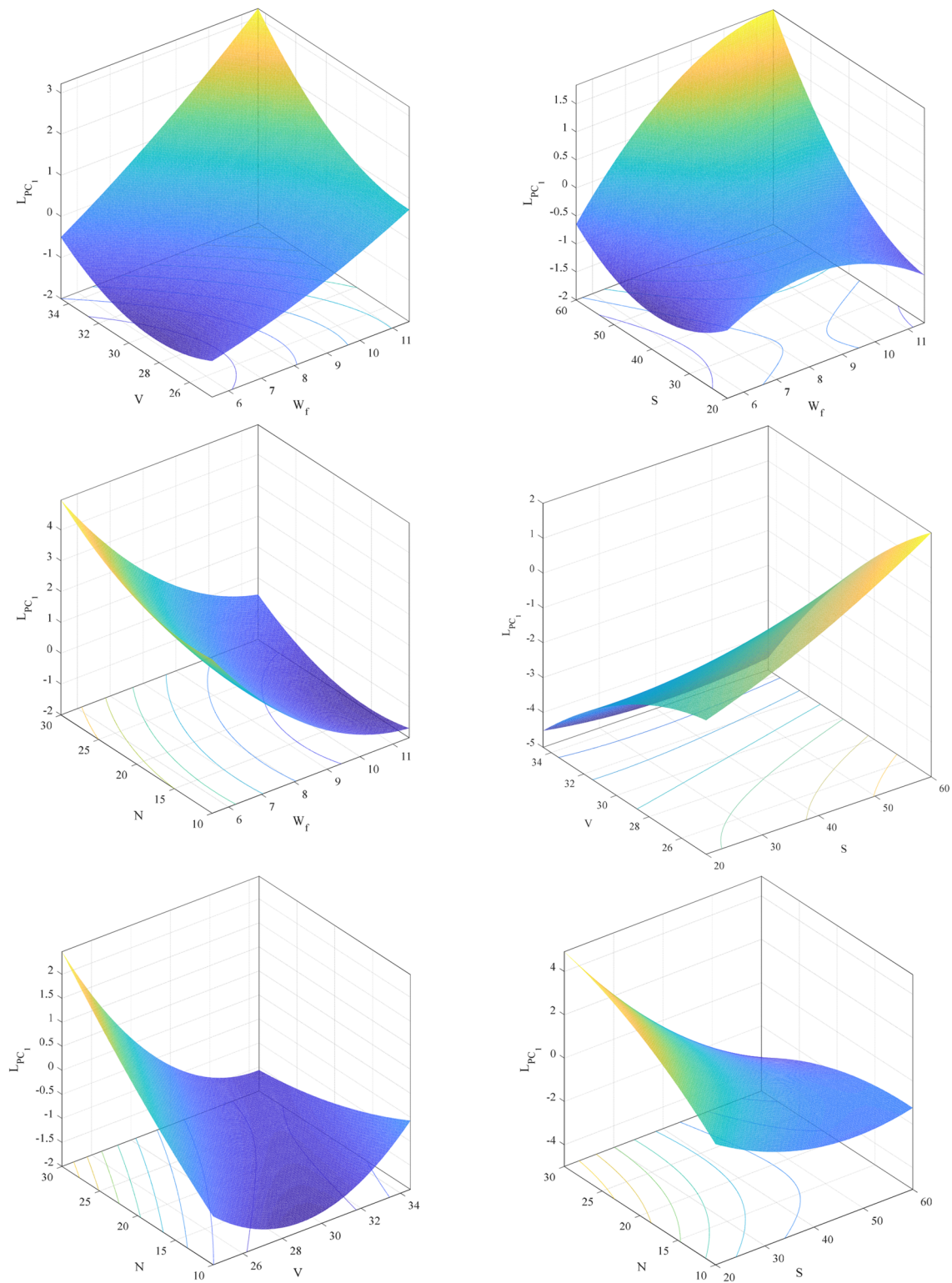


Fig. 4 Response surface graphic for L_{PC1}

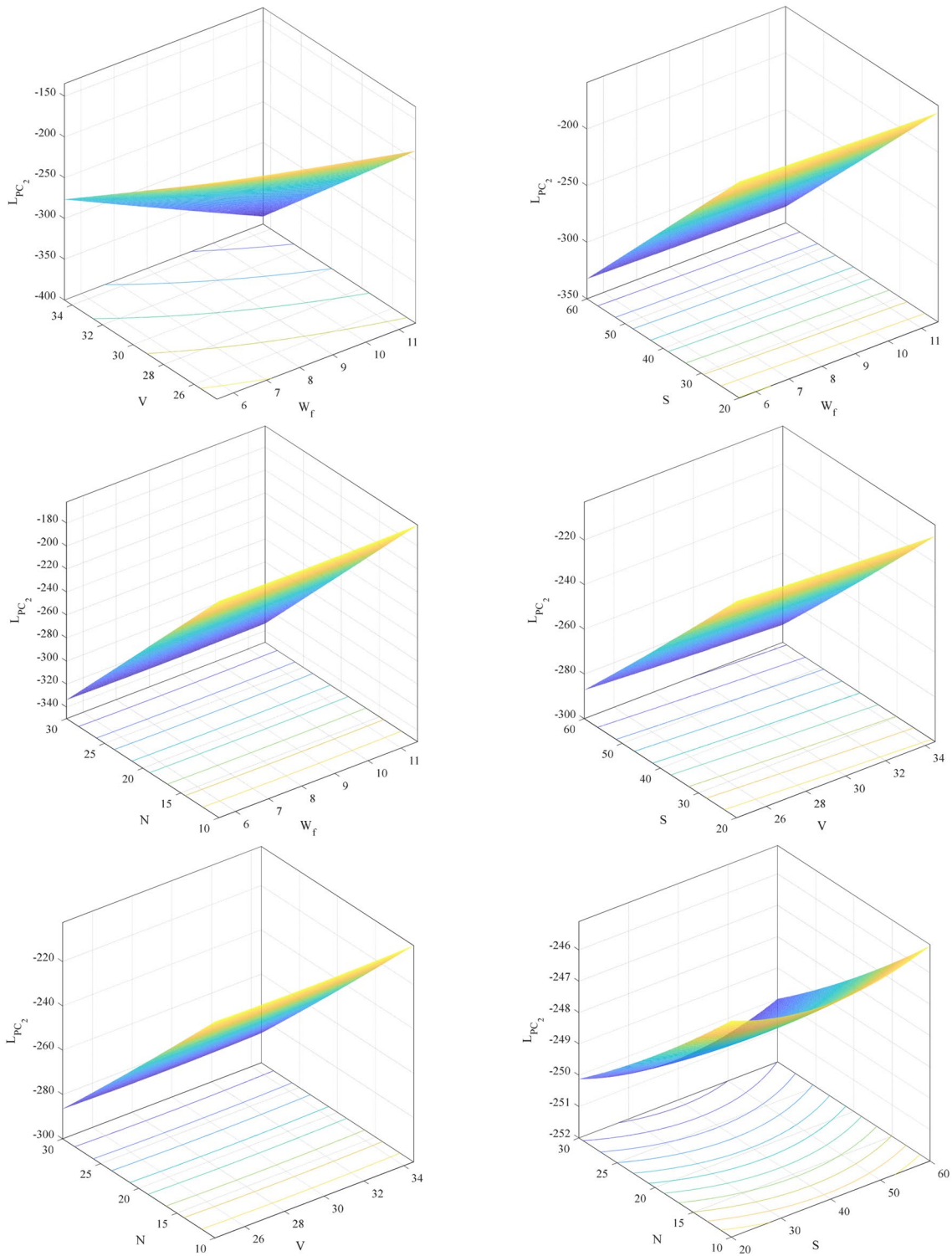


Fig. 5 Response surface graphic for L_{PC2}

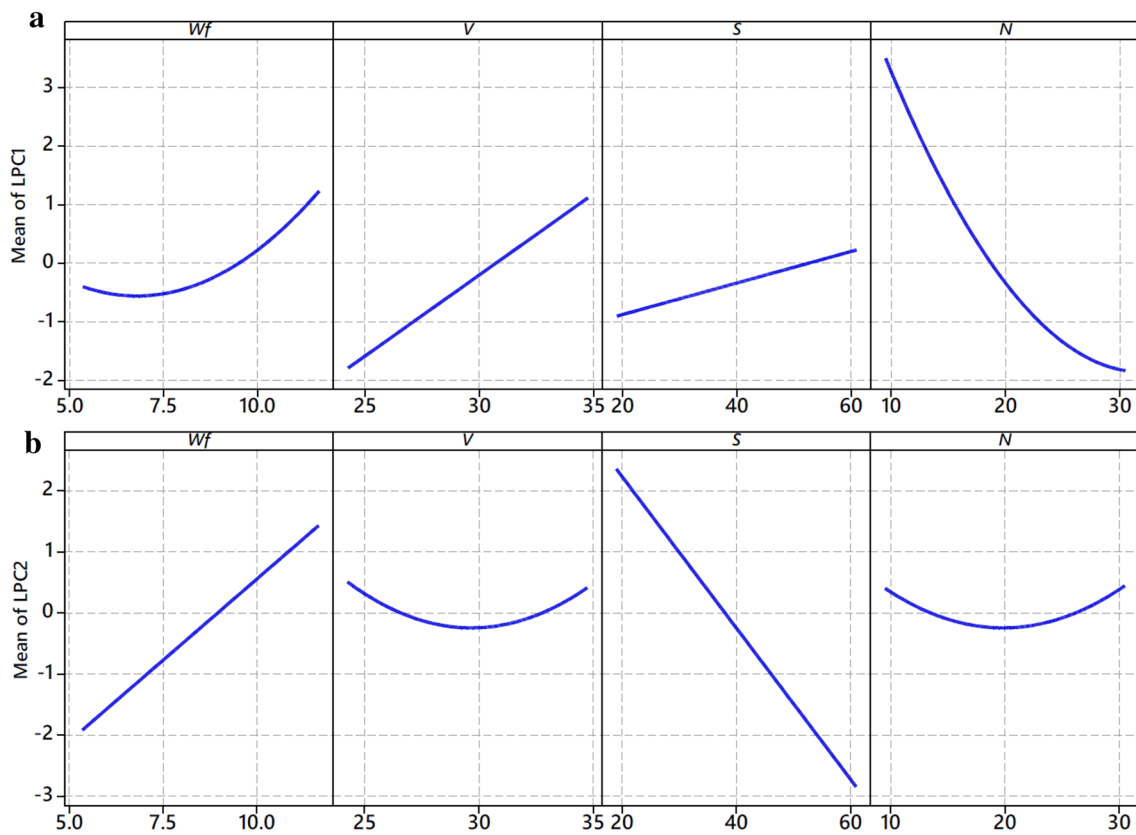


Fig. 6 Main effects plot for a L_{PC1} and b L_{PC2}

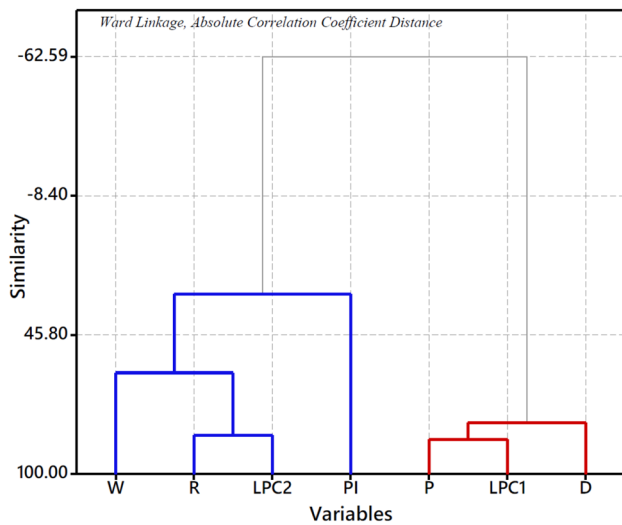


Fig. 7 Cluster analysis between the principal components of the loss function and the original responses

QLF, DOE, PCA and NBI. A case study using the flux-cored arc welding of stainless-steel cladding process was applied to validate this method. Finally, the following conclusions are presented:

- The multivariate Taguchi loss function optimization method presents a viable alternative to optimize quality responses, considering the loss functions calculated. In addition, the method presents an alternative for decision making at the optimum points of the Pareto frontier that consider the reduction of process costs;
- In the application of FCAW, the method presented an optimal value of $Y = [14.655 \text{ mm}; 0.959 \text{ mm}; 3.511 \text{ mm}; 18.03\%; 89.94\%]$ for W, P, R, D and PI, respectively. Such amounts represent a cost of US\$11.13, resulting in the best value of the Pareto frontier. These results also promote competitive advantages for the business, increasing the possibility of customer continuity and pro-

Table 7 Pareto frontier for the multivariate Taguchi loss function optimization approach

Run	w_1	Uncoded input variables				Uncoded responses and component scores							
		W_f	V	S	N	W	P	R	D (%)	PI (%)	L_{PC1}	L_{PC2}	
1	0.00	9.60	29.09	21.46	19.93	14.869	1.027	3.490	18.69	90.05	-1.1824	2.4986	
2	0.05	9.43	28.89	21.18	20.56	14.655	0.959	3.511	18.03	89.94	-1.3216	2.4909	
3	0.10	9.17	28.64	20.98	21.28	14.326	0.892	3.518	17.45	89.81	-1.4514	2.4538	
4	0.15	8.32	28.86	23.88	25.74	12.506	0.887	3.412	18.29	89.72	-1.4359	1.9668	
5	0.20	8.71	25.66	28.88	23.10	11.025	0.954	3.375	18.16	89.09	-1.4967	1.7165	
6	0.25	8.90	25.36	32.80	24.09	10.143	0.998	3.318	18.68	89.10	-1.5417	1.4168	
7	0.30	8.98	25.36	35.48	24.88	9.628	1.025	3.263	19.12	89.25	-1.6058	1.1763	
8	0.35	8.46	28.69	36.25	28.32	9.824	1.174	3.051	22.44	91.21	-1.5665	0.6158	
9	0.40	9.02	25.63	39.36	26.09	9.010	1.062	3.158	19.95	89.76	-1.7551	0.7609	
10	0.45	9.00	25.82	40.89	26.55	8.808	1.076	3.107	20.35	90.06	-1.8346	0.5684	
11	0.50	8.96	26.02	42.26	26.91	8.647	1.090	3.057	20.74	90.39	-1.9156	0.3804	
12	0.55	8.91	26.22	43.49	27.21	8.516	1.102	3.007	21.13	90.73	-1.9972	0.1942	
13	0.60	8.84	26.41	44.63	27.43	8.407	1.113	2.958	21.52	91.09	-2.0787	0.0077	
14	0.65	8.77	26.60	45.69	27.58	8.315	1.123	2.909	21.90	91.45	-2.1594	-0.1812	
15	0.70	8.68	26.78	46.70	27.67	8.235	1.132	2.861	22.29	91.81	-2.2387	-0.3745	
16	0.75	8.58	26.95	47.67	27.69	8.166	1.139	2.812	22.68	92.18	-2.3159	-0.5745	
17	0.80	8.47	27.11	48.62	27.66	8.104	1.144	2.762	23.08	92.56	-2.3899	-0.7842	
18	0.85	8.35	27.27	49.55	27.56	8.051	1.148	2.711	23.51	92.93	-2.4594	-1.0078	
19	0.90	8.20	27.44	50.50	27.38	8.004	1.151	2.656	23.98	93.32	-2.5221	-1.2525	
20	0.95	8.03	27.61	51.48	27.10	7.964	1.152	2.596	24.54	93.73	-2.5733	-1.5327	
21	1.00	7.80	27.83	52.61	26.61	7.932	1.152	2.520	25.29	94.19	-2.5993	-1.8912	

Bold: Optimal point found by the TLF method

Table 8 Information used to estimate costs

Information	Symbol	Value	Unit
Occupational factor	θ	0.65	-
Machine and labor cost per hour	C_{mlh}	200.00	US\$
Linear density of the wire	ρ_w	7.21	g/m
Wire reel cost per kg	C_w	73.80	US\$
Gas inflow	G_f	16.00	L/min
Gas price per m ³	G_p	698.48	US\$
Average energy price	P_e	0.35	US\$
Electrical efficiency of the equipment	E_e	0.7	-

Table 9 Equations of the costs included in C_t . Adapted from [19]

Cost	Symbol	Equation
Machine and labor	C_{ml}	$C_{ml} = \frac{t_w}{(3,600 \times \theta)} C_{mlh}$
Metal and flux	C_{mf}	$C_{mf} = \frac{W_f \times t_w \times \rho \times C_w}{(60,000)}$
Gas	C_g	$C_g = \frac{G_f \times t_w \times P_g}{60,000}$
Energy	C_e	$C_e = \frac{V \times I \times t_w \times P_e}{E_e}$

moting a better company reputation as well as increase in market participation.

- The method also provides an emphasis on quality characteristics based on the customer’s interest, where the target

values may vary based on the customer’s objective. In this sense, the benefits from optimization are translated into higher quality and lower costs from the customer’s point of view.

- The use of the PCA strategy allowed to reduce the data dimension, in addition to considering the existing variance–covariance structure in the data set. Combined with

Table 10 Cost, loss function and TLF values calculated for the Pareto frontier

Run	w_1	Cost (δ)		Loss function					TLF
		US\$		L_W	L_P	L_R	L_D	L_{PI}	
1	0.00	\$	11.08	0.350	0.520	0.075	0.040	0.110	1.095
2	0.05	\$	11.13	0.598	0.222	0.098	0.021	0.113	1.052
3	0.10	\$	11.14	1.108	0.052	0.106	0.010	0.116	1.391
4	0.15	\$	9.95	5.997	0.039	0.015	0.025	0.105	6.181
5	0.20	\$	8.71	11.559	0.162	0.003	0.019	0.104	11.847
6	0.25	\$	7.76	14.679	0.263	0.001	0.028	0.092	15.064
7	0.30	\$	7.16	16.242	0.326	0.013	0.036	0.083	16.699
8	0.35	\$	6.61	14.013	0.941	0.166	0.155	0.051	15.326
9	0.40	\$	6.37	17.613	0.412	0.063	0.053	0.067	18.208
10	0.45	\$	6.09	17.875	0.445	0.099	0.062	0.060	18.541
11	0.50	\$	5.84	17.988	0.476	0.141	0.072	0.054	18.731
12	0.55	\$	5.63	18.006	0.504	0.187	0.082	0.048	18.827
13	0.60	\$	5.45	17.964	0.528	0.238	0.092	0.043	18.865
14	0.65	\$	5.29	17.883	0.548	0.294	0.103	0.039	18.867
15	0.70	\$	5.14	17.776	0.564	0.354	0.114	0.034	18.843
16	0.75	\$	5.01	17.653	0.575	0.419	0.126	0.031	18.804
17	0.80	\$	4.89	17.515	0.582	0.489	0.139	0.027	18.753
18	0.85	\$	4.78	17.364	0.584	0.567	0.154	0.024	18.693
19	0.90	\$	4.68	17.197	0.581	0.654	0.171	0.021	18.625
20	0.95	\$	4.58	17.006	0.573	0.759	0.192	0.018	18.548
21	1.00	\$	4.47	16.758	0.558	0.900	0.224	0.015	18.456

Bold: Optimal point found by the TLF method

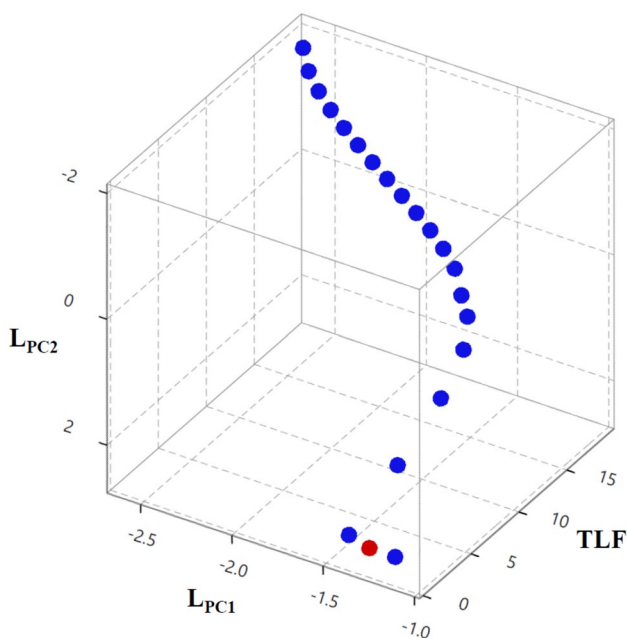


Fig. 8 Relationship between the Pareto frontier and the total loss function

the NBI technique, PCA promoted a minimization of 90% of the optimization subproblems (210–21 subproblems), reducing the computational effort required for this application.

- The comparison with results from another study in the literature, made it possible to infer that the proposed method presented better performance when considering the cost of the process. The results showed that the loss-based approach provided results with less deviation from the targets, in addition to promoting less total loss. The TLF decision-making method proved to be a valid option to find the best point on a Pareto frontier for industrial applications and can be extended to other segments.

Finally, as suggestions for future studies, the proposed method can be extended to stochastic applications, as well as the use of other optimization and multivariate techniques. In addition, the TLF strategy can be applied to decision making related to other processes.

Table 11 Comparison of studies based on optimal values and TLF decision maker

	Cost (δ)	W	P	R	D	PI	TLF
Target		15.57	0.83	3.34	16.27	100	
Gomes et al. [23]	\$ 5.30	11.9	0.92	3.33	16.61	88.73	4.7011
Proposed method	\$ 11.13	14.66	0.96	3.51	18.03	89.94	1.0521
Unit	[US\$]	[mm]	[mm]	[mm]	[%]	[%]	

Bold: best values for each column

Acknowledgements The authors would like to express their gratitude to Prof. M.Sc. Alexandre Fonseca Torres, CAPES, FAPEMIG (Grant number APQ-00385-18) and CNPq (project number 303586/2015-0 and 409318/2017-5) for their support in this research.

References

- Chatterjee S, Mahapatra SS, Bharadwaj V et al (2019) Prediction of quality characteristics of laser drilled holes using artificial intelligence techniques. *Eng Comput*. <https://doi.org/10.1007/s00366-019-00878-y>
- Gomes GF, de Almeida FA, de Lopes AP et al (2019) A multiobjective sensor placement optimization for SHM systems considering Fisher information matrix and mode shape interpolation. *Eng Comput* 35:519–535. <https://doi.org/10.1007/s00366-018-0613-7>
- Cicconi P, Castorani V, Germani M et al (2020) A multi-objective sequential method for manufacturing cost and structural optimization of modular steel towers. *Eng Comput* 36:475–497. <https://doi.org/10.1007/s00366-019-00709-0>
- Keshtiarra M, Golabi S, Tarkesh Esfahani R (2019) Multi-objective optimization of stainless steel 304 tube laser forming process using GA. *Eng Comput*. <https://doi.org/10.1007/s00366-019-00814-0>
- Daroz Gaudêncio JH, de Almeida FA, Turrioni JB et al (2019) A multiobjective optimization model for machining quality in the AISI 12L14 steel turning process using fuzzy multivariate mean square error. *Precis Eng* 56:303–320. <https://doi.org/10.1016/j.precisioneng.2019.01.001>
- Thomas L (1999) The Taguchi loss function. *Work Study* 48:218–223. <https://doi.org/10.1108/00438029910286477>
- Taguchi G, Elsayed EATH (1989) *Quality engineering in production systems*. McGraw-Hill, New York
- Wang B, Moayedi H, Nguyen H et al (2019) Feasibility of a novel predictive technique based on artificial neural network optimized with particle swarm optimization estimating pullout bearing capacity of helical piles. *Eng Comput*. <https://doi.org/10.1007/s00366-019-00764-7>
- Li E, Zhou J, Shi X et al (2020) Developing a hybrid model of salp swarm algorithm-based support vector machine to predict the strength of fiber-reinforced cemented paste backfill. *Eng Comput*. <https://doi.org/10.1007/s00366-020-01014-x>
- Ferreira Gomes G, Souza Chaves JA, de Almeida FA (2020) An inverse damage location problem applied to AS-350 rotor blades using bat optimization algorithm and multiaxial vibration data. *Mech Syst Signal Process* 145:106932. <https://doi.org/10.1016/j.ymssp.2020.106932>
- Gomes GF, de Almeida FA, Ancelotti AC, da Cunha SS (2020) Inverse structural damage identification problem in CFRP laminated plates using SFO algorithm based on strain fields. *Eng Comput*. <https://doi.org/10.1007/s00366-020-01027-6>
- Ribeiro Junior RF, de Almeida FA, Gomes GF (2020) Fault classification in three-phase motors based on vibration signal analysis and artificial neural networks. *Neural Comput Appl*. <https://doi.org/10.1007/s00521-020-04868-w>
- Yu Z, Shi X, Zhou J et al (2020) Prediction of blast-induced rock movement during bench blasting: use of gray wolf optimizer and support vector regression. *Nat Resour Res* 29:843–865. <https://doi.org/10.1007/s11053-019-09593-3>
- Belinato G, de Almeida FA, de Paiva AP et al (2019) A multivariate normal boundary intersection PCA-based approach to reduce dimensionality in optimization problems for LBM process. *Eng Comput* 35:1533–1544. <https://doi.org/10.1007/s00366-018-0678-3>
- Almeida FA, Leite RR, Gomes GF et al (2020) Multivariate data quality assessment based on rotated factor scores and confidence ellipsoids. *Decis Support Syst* 129:113173. <https://doi.org/10.1016/j.dss.2019.113173>
- Nhu V-H, Samui P, Kumar D et al (2019) Advanced soft computing techniques for predicting soil compression coefficient in engineering project: a comparative study. *Eng Comput*. <https://doi.org/10.1007/s00366-019-00772-7>
- de Almeida FA, Miranda Filho J, Amorim LF et al (2020) Enhancement of discriminatory power by ellipsoidal functions for substation clustering in voltage sag studies. *Electr Power Syst Res* 185:106368. <https://doi.org/10.1016/j.epsr.2020.106368>
- Shirani Faradonbeh R, Taheri A (2019) Long-term prediction of rockburst hazard in deep underground openings using three robust data mining techniques. *Eng Comput* 35:659–675. <https://doi.org/10.1007/s00366-018-0624-4>
- Marques PV, Modenesi PJ, Bracarense AQ (2017) *Soldagem: fundamentos e tecnologia*, 4th edn. Elsevier, Rio de Janeiro
- Torres AF, Rocha FB, Almeida FA et al (2020) Multivariate stochastic optimization approach applied in a flux-cored arc welding process. *IEEE Access* 8:61267–61276. <https://doi.org/10.1109/ACCESS.2020.2983566>
- Choi D, Lee H, Cho S-K et al (2020) Microstructure and charpy impact properties of FCAW and SAW heat affected zones of 100 mm thick steel plate for offshore platforms. *Met Mater Int* 26:867–881. <https://doi.org/10.1007/s12540-020-00626-8>
- Cheng F, Zhang S, Di X et al (2017) Arc characteristic and metal transfer of pulse current horizontal flux-cored arc welding. *Trans Tianjin Univ* 23:101–109. <https://doi.org/10.1007/s12209-017-0039-0>
- Gomes JHF, Paiva AP, Costa SC et al (2013) Weighted Multivariate Mean Square Error for processes optimization: a case study on flux-cored arc welding for stainless steel claddings. *Eur J Oper Res* 226:522–535. <https://doi.org/10.1016/j.ejor.2012.11.042>
- Senthilkumar B, Kannan T, Madesh R (2017) Optimization of flux-cored arc welding process parameters by using genetic algorithm. *Int J Adv Manuf Technol* 93:35–41. <https://doi.org/10.1007/s00170-015-7636-7>
- Ordoobadi SM (2013) Application of AHP and Taguchi loss functions in evaluation of advanced manufacturing technologies. *Int J Adv Manuf Technol* 67:2593–2605. <https://doi.org/10.1007/s00170-012-4676-0>

26. Myers RH, Montgomery DC, Anderson-Cook CM (2016) Response surface methodology: process and product optimization using designed experiments, 4th edn. Wiley, New York
27. Echempati R, Fox A (2013) Integrated metal forming and vibration analysis of sheet metal parts. *Eng Comput* 29:307–318. <https://doi.org/10.1007/s00366-012-0273-y>
28. Simpson TW, Poplinski JD, Koch PN, Allen JK (2001) Metamodels for computer-based engineering design: survey and recommendations. *Eng Comput* 17:129–150. <https://doi.org/10.1007/PL00007198>
29. Antony J (2000) Multi-response optimization in industrial experiments using Taguchi's quality loss function and principal component analysis. *Qual Reliab Eng Int* 16:3–8. [https://doi.org/10.1002/\(SICI\)1099-1638\(200001/02\)16:1%3c3:AID-QRE276%3e3.0.CO;2-W](https://doi.org/10.1002/(SICI)1099-1638(200001/02)16:1%3c3:AID-QRE276%3e3.0.CO;2-W)
30. Johnson RA, Wichern D (2007) Applied multivariate statistical analysis, 6th edn. Prentice-Hall, New Jersey
31. Gu F, Hall P, Miles NJ (2016) Performance evaluation for composites based on recycled polypropylene using principal component analysis and cluster analysis. *J Clean Prod* 115:343–353. <https://doi.org/10.1016/j.jclepro.2015.12.062>
32. Salah B, Zoheir M, Slimane Z, Jurgen B (2015) Inferential sensor-based adaptive principal components analysis of mould bath level for breakout defect detection and evaluation in continuous casting. *Appl Soft Comput* 34:120–128. <https://doi.org/10.1016/j.asoc.2015.04.042>
33. de Almeida FA, Gomes GF, Gaudêncio JHD et al (2019) A new multivariate approach based on weighted factor scores and confidence ellipses to precision evaluation of textured fiber bobbins measurement system. *Precis Eng* 60:520–534. <https://doi.org/10.1016/j.precisioneng.2019.09.010>
34. Das I, Dennis JE (1998) Normal-boundary intersection: a new method for generating the pareto surface in nonlinear multicriteria optimization problems. *SIAM J Optim* 8:631–657. <https://doi.org/10.1137/S1052623496307510>
35. Ahmadi A, Moghimi H, Nezhad AE et al (2015) Multi-objective economic emission dispatch considering combined heat and power by normal boundary intersection method. *Electr Power Syst Res* 129:32–43. <https://doi.org/10.1016/j.epsr.2015.07.011>
36. Izadbakhsh M, Gandomkar M, Rezvani A, Ahmadi A (2015) Short-term resource scheduling of a renewable energy based micro grid. *Renew Energy* 75:598–606. <https://doi.org/10.1016/j.renene.2014.10.043>
37. Mavalizadeh H, Ahmadi A (2014) Hybrid expansion planning considering security and emission by augmented epsilon-constraint method. *Int J Electr Power Energy Syst* 61:90–100. <https://doi.org/10.1016/j.ijepes.2014.03.004>

Publisher's Note Springer Nature remains neutral with regard to jurisdictional claims in published maps and institutional affiliations.